DEM modeling of unsaturated geomaterials for predicting resilient modulus

Hyun-Su Park & Seong-Wan Park
Dankook University, Gyeonggi-do, Republic of Korea

ABSTRACT: Soil suction and the degree of saturation influence the resilient modulus. A suction stress model that incorporates both suction and degree of saturation can be applied to the resilient modulus. To evaluate the effect of suction stress on resilient modulus, water effects were categorized into bulk and meniscus water, and cyclic loading was applied to the samples. The soil water characteristic curve (SWCC) was generated using discrete element method (DEM) analysis. Additionally, the resilient modulus was observed to vary with both deviator stress and the degree of saturation. The trends observed in this study are consistent with the results of other researchers. These findings demonstrate that the water division and cyclic loading algorithm effectively represent the unsaturated soil state, and DEM analysis revealed that suction stress influences the resilient modulus, with the resilient modulus increasing as suction stress increased.

1 INTRODUCTION

The resilient modulus is widely used to understand the stiffness of pavement foundations and is influenced by changes in suction. The relationship between suction and resilient modulus can be reasonably predicted by considering the moisture regime (Han & Vanapalli, 2016). Suction stress, derived from suction and effective saturation, is used to predict shear strength in unsaturated soil mechanics (Karube et al., 1986).

Various tests can be used to evaluate the effect of suction on the resilient modulus. However, these methods have limitations, including user-dependency, limited to specific suction ranges and time-consumption. Recently, discrete element method (DEM) analysis has been used to overcome the limitations of laboratory tests in unsaturated soil materials (Liu & Sun, 2002; Li et al., 2018).

This study simulates the behavior of unsaturated soil under cyclic loading using DEM analysis (PFC 3D). The unsaturated soil modeling method using DEM analysis was proposed, and the resilient modulus test using the flexible membrane was performed using the proposed unsaturated soil modeling method. From these results, a soil-water characteristic curve (SWCC) and resilient modulus at 5 cycles were generated through DEM simulation, and the effect of suction stress on resilient modulus was evaluated.

2 UNSATURATED STATE THROUGH DEM

2.1 *Definition of suction stress*

Suction stress is related to both suction and the degree of saturation and has been evaluated under various stress conditions (Karube and Kato, 1994). It is defined as the sum of bulk and meniscus stress, where bulk stress refers to the stress imposed on pores filled with water, and meniscus stress refers to the stress imposed by the capillary force. Suction stress can be calculated as follows:

$$p_s = p_m + p_b = (S_r - S_{r0})/(1 - S_{r0}) \cdot s \qquad (1)$$

where p_m = the meniscus stress, p_b = the bulk stress, S_r = the degree of saturation, S_{r0} = the residual degree of saturation, and s = the matric suction.

2.2 *Modelling of unsaturated state in DEM analysis*

The unsaturated state was modeled through three stages of DEM analysis. First, the volume of water for particle-to-particle interaction was defined based on the spacing between particles, as shown in Figure 1. Second, Bulk water was defined as the water overlapping within the triangle area formed by three particles, while the remaining water was classified as meniscus water. Finally, the capillary force calculated using the general capillary force method was applied to meniscus water, and the capillary force calculated

using the boundary method was applied to bulk water (Hotta et al., 1974).

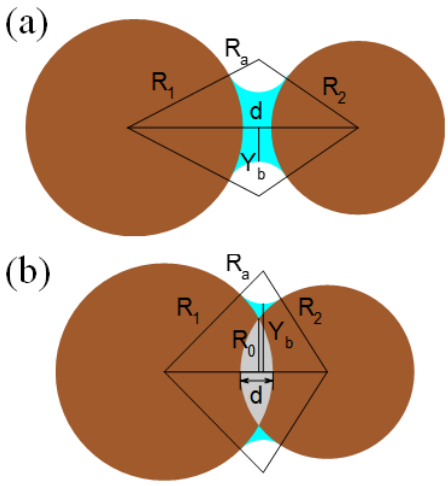

Figure 1 Water volume calculation method: (a) when the particles are separated: (b) when the particles overlap

3 RESILIENT MODULUS TEST MODELING

The confining stress was applied to the membrane particles using the membrane modeling algorithm (Li et al., 2017). Deviator stress with a haversine shape was applied to the wall boundary with deformation control. Additionally, the applied particle size distribution is shown in Figure 2, and the smallest particle size was adjusted to reduce simulation time. The soil particles have a spherical shape, and their diameters range from 0.3031 mm to 2.0 mm. The density of specimen was considered using density modeling method proposed by Chang et al. (2017) to account for discrepancy in particle shape and particle size distribution compared to real particles.

The maximum and minimum void ratios obtained from the density modeling method are 0.417 and 0.360, respectively. The void ratio of specimen was set to 0.360, which corresponds to 100 % relative density. The specimen was compacted to achieve this void ratio of 0.360. The membrane surrounding the specimen was then modeled using spherical particles (membrane balls). The membrane ball size was selected to match the smallest particle size of specimen to ensure computational efficiency and accuracy.

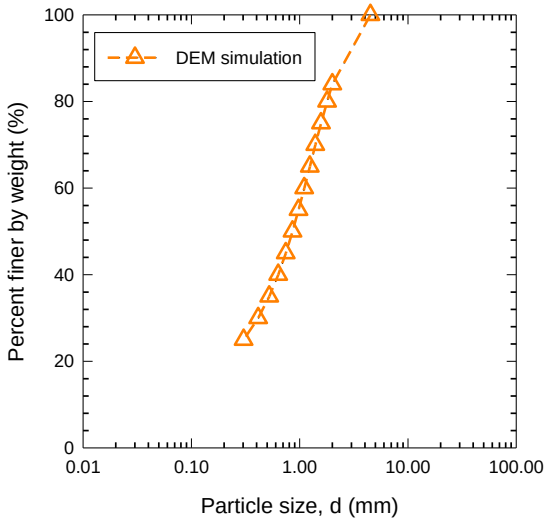

Figure 3 Particle size distribution

In resilient modulus test, the AASHTO manual specifies that the confining pressure for fine-grained subgrade materials ranges from 27.6 kPa to 82.8 kPa, while the cyclic stress ranges from 27.6 kPa to 96.6 kPa. This paper aims to evaluate the DEM modeling algorithm in resilient modulus tests for unsaturated soil. Accordingly, the confining pressure was set to 27.6 kPa, and the cyclic stress was varied from 13.8 kPa to 68.9 kPa. Additionally, to assess changes in the resilient modulus under different degree of saturation, the degree of saturation was varied from 1 % to 99 %. Moreover, because the suction stress exhibits a sharp change at high suction levels and decrease markedly beyond approximately 5 % saturation as shown in figure 3, the change in the resilient modulus under low saturation levels was evaluated in detail.

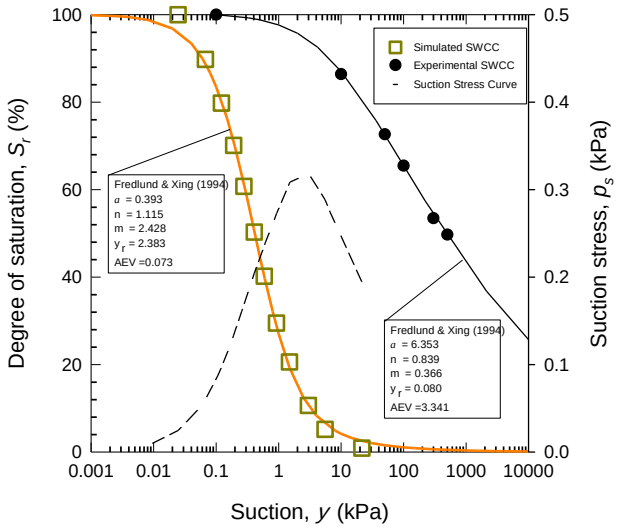

Figure 2 Soil-water characteristic curve generated through DEM analysis

The contact properties of membrane particles, and specimen particles are summarized in Table 1. The effective modulus of the specimen particles is set to 6,000 kN/m, and the effective modulus of membrane particles is set to one-tenth the effective modulus of the specimen particles. If the effective modulus of membrane particles is too small, the membrane particles may penetrate into the specimen. Therefore, the effective modulus of membrane particles was determined through a trial-and-error approach.

4 SWCC AND RESILIENT MODULUS AT VARIOUS SUCTIONS

Suction was calculated based on the water distribution between particles using the proposed unsaturated soil modeling method. Consequently, the relationship between suction and degree of saturation (S_r), referred to as the soil-water characteristic curve (SWCC), was

generated through DEM simulations, as shown in Figure 3. The generated SWCC includes key characteristics such as the air entry value (AEV) and residual suction. These results reveals that the shape of the generated SWCC closely resembles those obtained from laboratory tests.

Table 1. Contact model properties

Parameters	Value
Membrane particles	
Effective modulus (kN/m)	600
Normal to shear stiffness ratio	0
Friction coefficient	0
Damping ratio	0.7
Density (kg/m^3)	1
Specimen particles	
Effective modulus (kN/m)	6000
Normal to shear stiffness ratio	1.2
Friction coefficient	0.5
Damping ratio	0.7
Density (kg/m^3)	2.69
Maximum void ratio, e_{max}	0.417
Minimum void ratio, e_{min}	0.360
Target viod ratio, e	0.360
Relative density, Dr (%)	100

Figure 4 illustrates the changes in bulk and meniscus water with the degree of saturation. The ratio of bulk to meniscus water changes significantly at approximately 25% saturation. Additionally, when the total degree of saturation surpasses 20%, the amount of meniscus water remains nearly constant, and there is negligible variation at degree of saturation below approximately 10%. Meniscus water remained at approximately 10% of the degree of saturation, as reported by Karube & kawai (2001), and exhibited behavior consistent with that shown in Figure 4.

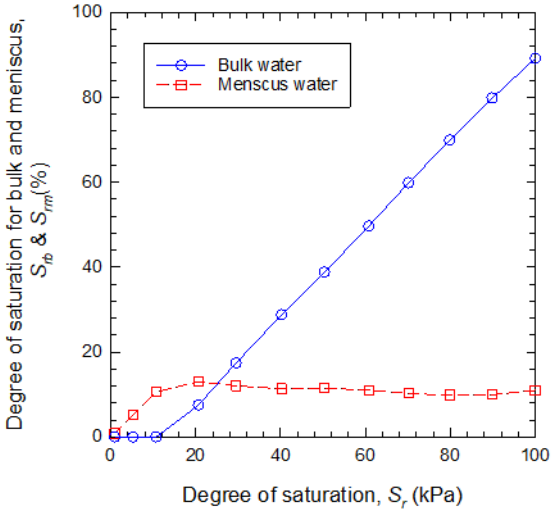

Figure 4 Changes in bulk and meniscus water with respect to the degree of saturation

Therefore, the proposed water division model for bulk and meniscus water aligns with the laboratory test results.

The difference in resilient modulus is minimal because the effective modulus of the particles was set to a small value to reduce the computational time. Table 2 presents the maximum and minimum resilient moduli for varying deviator stress levels. The maximum and minimum resilient modulus values were selected based on the values obtained by varying the degree of saturation. Since the difference in resilient modulus with changes in the degree of saturation are minimal, the resilient modulus was normalized using its maximum and minimum values. Figure 5 illustrates the relationship between the degree of saturation and the normalized resilient modulus. This normalization scaled the resilient modulus to a range between 0 and 1. The resilient modulus decreases as the deviator stress increases. This trend is consistent with previous findings that the resilient modulus decreases with increasing deviator stress (Ng et al., 2013; Han and Vanapalli, 2016). Additionally, the resilient modulus increases as the degree of saturation decreases, with the slope decreasing at low saturation, as illustrated in Figure 5 (Banerjee et al., 2020).

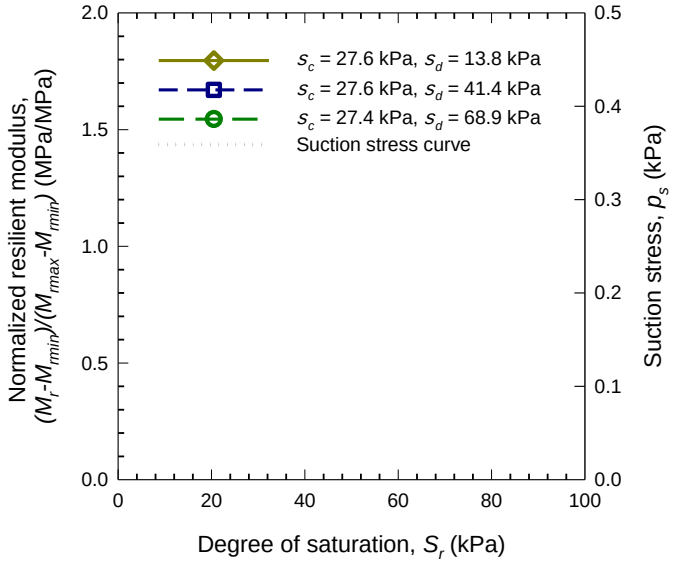

Figure 5 Changes in normalized resilient modulus with respect to the degree of saturation

Table 2 Maximum and minimum resilient modulus

No.	1	2	3
Confining stress (kPa)	27.6	27.6	27.6
Deviator stress (kPa)	13.8	41.4	68.9
Maximum resilient modulus modulus (MPa)	4.10	3.93	3.30
Minimum resilient modulus (MPa)	4.09	3.88	3.06

There was the relationship between the resilient modulus and degree of saturation and the relationship between suction stress and degree of saturation in figure 5. Suction stress was calculated using Eq. (1) based on the generated SWCC.

At high saturation, suction stress increased as the degree of saturation decreased. However, at low saturation of approximately 10 %, the suction stress decreased as the degree of saturation increased. This behavior occurs because, at low degree of saturation, the water volume is relatively small, resulting in suction stress decreasing as the degree of saturation increases. However, at deviator stress of 13.8 kPa and 41.4 kPa, the resilient modulus increases with the degree of saturation. This is attributed to the differences in deviator stress. In this paper, the resilient modulus was calculated at 5 cycles due to the simulation time constraints, as each cycle requires approximately 5 days. Therefore, while the resilient modulus converged within 5 cycles at deviator stress of 68.1 kPa, it did not converge within 5 cycles at lower deviator stresses (i.e., 13.8 kPa and 41.4 kPa), resulting in an increase in the resilient modulus as the degree of saturation increases.

When the relationship between the degree of saturation and suction stress was compared with the normalized resilient modulus results, the resilient modulus at a deviator stress of 68.9 kPa demonstrated a strong correlation with suction stress. However, under other deviator stress conditions, the resilient modulus increased with suction stress but a substantial portion of the increase occurred at low saturation. This behavior is attributed to the applied meniscus water contact force exceeding that of bulk water. These results indicate that the resilient modulus is closely related to suction stress.

5 CONCLUSIONS

This study categorized the water contents into bulk and meniscus water to simulate unsaturated soils. Cyclic loading was applied to a specimen composed of bulk and meniscus water, and the resilient modulus was obtained from these simulations.

Based on the particle size distribution, the SWCC was generated through DEM simulation. Bulk water was dominant at a saturation above 25%, whereas meniscus water was dominant below 25%. These results demonstrate that the unsaturated soil state can be effectively simulated using DEM analysis despite its limitations. Additionally, the resilient modulus was obtained through DEM simulation and decreased as the deviator stress increased from 13.8 kPa to 68.9 kPa. Finally, the suction stress was compared with the resilient modulus. The trend of suction stress with the degree of saturation changed, whereas particle displacement changed at 5% saturation. Although the relationship between suction stress and resilient modulus remains unclear due to DEM simulation limitations, suction stress was found to influence the resilient modulus.

ACKNOLEDGMENT

This work was supported by the National Research Foundation of Korea (NRF) grant funded by the Korea government (MSIT) (No. RS-2023-00221184)

REFERENCES

Banerjee, A., Puppala, A.J., Hoyos, L.R., Likos, W.J., & Patil, U.D. 2020. Resilient Modulus of Expansive Soils at High Suction Using Vapor Pressure Control. *Geotechnical Testing Journal* 43(3): 720-736. https://doi.org/10.1520/GTJ20180255

Chang, C.S. Deng, Y., & Yang, Z. 2017. Modeling of Minimum Void Ratio for Granular Soil with Effect of Particle Size Distribution. *Journal of Engineering Mechanics* 143(9): 04017060. https://doi.org/10.1061/(ASCE)EM.1943-7889.0001 270

De Bono, J. McDowell, G., & Wanatowski, D. 2012. Discrete element modelling of a flexible membrane for triaxial testing of granular material at high pressures. *Géotechniqu Letters* 2(4): 199-203. https://doi.org/10.1680/geolett.12.00040

Fredlund, D.G., & Xing, A. 1994. Equations for the soil-water characteristic curve. *Canadian Geotechnical Journal* 31(4): 521-532. https://doi.org/10.1139/t94-061

Han, Z., & Vanapalli, S.K. 2016. State-of-the-art: Prediction of Resilient Modulus of Unsaturated Subgrade Soils. *International Journal of Geomechanics* 16(4): 04015104. https://doi.org/10.1061/(ASCE)GM.1943-5622.0000631

Hotta, K., Takeda, K., & Iionya, K. 1974. The capillary binding force of a liquid bridge, *Powder Technology*, 10: 231-242. https://doi.org/10.1016/0032-5910(74)85047-3

Karube, D., Kato, S., & Katsuyama, J. 1986. Effective stress and soil constants of unsaturated kaolin. *Doboku Gakkai Ronbunshu* 370(5): 179-188. (In Japanese) https://doi.org/10.2208/jscej.1986.370_179

Karube, D. & Kato, S. 1994. An ideal unsaturated soil and the Bishop's soil. *In Proceedings of 13th international conference on conference on soil mechanics and foundations engineering*, New Delhi, India.

Karube, D. & Kawai, K. 2001. The role of pore water in the mechanical behavior of unsaturated soils. *Geotechnical and Geological Engineering* 19: 211-241. https://doi.org/10.1023/A:1013188200053

Li, Z., Wang, Y.H., Ma, C.H., & Mok, C.M.B. 2017. Experimental characterization and 3D DEM simulation of bond breakages in artificially cemented sands with different bond strengths when subjected to triaxial shearing. *Acta Geotechnical* 12: 987-1002. https://doi.org/10.1007/s11440-017-0593-6

Li, T., Jiang M., & Thornton. 2018. Three-dimensional discrete element analysis of triaxial tests and wetting tests on unsaturated compacted silt. *Computers and Geotechnics* 97: 90-102. https://doi.org/10.1016/j.compgeo.2017.12.011

Liu, S.H., & Sun, D.A. 2002. Simulating the collapse of unsaturated soil by DEM. *International Journal for Numerical and Analytical Methods in Geomechanics* 26: 633-646. https://doi.org/10.1002/nag.215

Ng, C.W.W., Zhou, C., Yuan, Q., & Xu, J. 2013. Resilient modulus of unsaturated subgrade soil: experimental and theoretical investigations. *Canadian Geotechnical Journal* 50(2): 223-232. https://doi.org/10.1139/cgj-2012-0052